frontiers | Frontiers in Environmental Science

TYPE Original Research
PUBLISHED 12 October 2022
DOI 10.3389/fenvs.2022.1017809

OPEN ACCESS

EDITED BY
Ling Xia,
Wuhan University of Technology, China

REVIEWED BY
Hongmei Deng,
Guangzhou University, China
Chandra Sekhar Gahan,
Central University of Rajasthan, India

*CORRESPONDENCE
Xiaowen Liu,
liuxiaowen@scies.org

SPECIALTY SECTION
This article was submitted to Toxicology, Pollution and the Environment, a section of the journal Frontiers in Environmental Science

RECEIVED 12 August 2022
ACCEPTED 30 August 2022
PUBLISHED 12 October 2022

CITATION
Tong L, Peng X, Chen D, Chen Y, Wen Y, Wang W and Liu X (2022), Characterization and risk assessment of soil around waste rock heaps affected by acid rock drainage in an abandoned pyrite mining area.
Front. Environ. Sci. 10:1017809.
doi: 10.3389/fenvs.2022.1017809

Characterization and risk assessment of soil around waste rock heaps affected by acid rock drainage in an abandoned pyrite mining area

Lizhi Tong[1], Xiangqin Peng[1], Di Chen[1], Yanzhi Chen[1], Yong Wen[1], Wei Wang[1,2] and Xiaowen Liu[1]*

[1]South China Institute of Environmental Sciences, Ministry of Ecology and Environment, Guangzhou, China, [2]School of Minerals Processing and Bioengineering, Central South University, Changsha, China

Acid rock drainage (ARD) is one of the most serious and potentially lasting environmental issues for the mining industry. Many researchers investigated the impact of ARD on downstream farmland, but few focused on the soil properties change around waste rock heaps. In this study, a total of 119 soil samples were taken around the 35 waste rock heaps which are scattered in 12 mining sites in an abandoned pyrite mining area (Baihe County, Northwest China). Both rainy and dry seasons of ARD were collected from the discharge outlet of each mining site. The bulk levels of potentially toxic elements (PTEs), including As, Cd, Cu, Ni, Cr, Zn, Pb, Fe, Mn, and F, in waste rock, soil, and ARD samples were analyzed. Leaching concentration and chemical speciation of these PTEs in soils were further investigated. The results show that the ARD had very high pollution loads of PTEs both in the rainy season and dry season, continuously exporting pollutants to the surrounding soils. More than 70% of the soil samples were acidic (pH<5.5). The bulk of As in 17 soil surface samples exceeded the risk control limit specified in China (60 mg/kg), while the leaching concentrations of As and other PTEs in soil were far below the regulated limits. According to the sequential extraction results, the residual fraction of As, Cr, Cu, Zn, and Ni in the soil accounted for over 90%, indicating these metals were possibly retained by the silicate matrix. Considering the relatively low bioavailability of PTEs and limited exposure routes, the human health risk of the soil surrounding the waste heap is generally acceptable. This research work provides a more comprehensive understanding of the properties and effects of ARD in the pyrite mining area which is conducive to the development of a sustainable control strategy of environmental pollution in typical mining regions.

KEYWORDS

acid rock drainage, waste rock heaps, soil quality, pollution load, pyrite mining area, environmental risk

Highlights

- The impact of acid rock drainage on soil around waste rock heaps was studied.
- Metal (loid)s with high pollution load were identified in acid rock drainage.
- Acidification and high As levels were found in soils around waste rock heaps.
- The residual fraction of As, Cr, Cu, Zn, and Ni in soils accounted for over 90%.
- Human health risk of the soils surrounding the waste heaps is acceptable.

1 Introduction

Historically intense mining of sulfide deposits worldwide has left a legacy of abandoned mining sites with numerous sulfide-bearing solid wastes, including topsoil overburden, waste rock, and tailings (Zhou et al., 2018; Casagrande et al., 2019; Alekseyev, 2022). The acid rock drainage (ARD) process initiates when pyrite (FeS_2) and other sulfide minerals (e.g., CuS) in mining wastes, are oxidized through complex biochemical reactions in the presence of oxygen, microorganisms (*Thiobacillus thiooxidans* and *Thiobacillus ferrooxidans*), and water (Naidu et al., 2019; Sulonen et al., 2021).

$$FeS_{2(s)} + 15/4\,O_{2(g)} + 7/2H_2O_{(l)} \rightarrow Fe(OH)_{3(s)} + 2SO_{4(aq)}^{2-} + 4H_{(aq)}^{+} \quad (1)$$

$$FeS_{2(s)} + 14Fe_{(aq)}^{3+} + 8H_2O_{(l)} \rightarrow 15Fe_{(aq)}^{2+} + 2SO_{4(aq)}^{2-} + 16H_{(aq)}^{+} \quad (2)$$

ARD is one of the most serious and potentially lasting environmental issues for the global mining industry (Fan et al., 2017; Ma et al., 2019). With elevated acidity and high content of sulfates and metals/metalloids, ARD can directly deteriorate downstream surface water and groundwater environment (Plaza et al., 2017; Plaza et al., 2018). Besides, the use of acidic water for agricultural irrigation further leads to elevated or excessive metal concentrations in the soil system and surrounding vegetation (Olenici et al., 2017). On one hand, the minerals are usually accompanied by various potentially toxic trace metals (PTEs) such as Pb, Cd, Cr, Mn, Ni, Cu, Tl, and Zn (Liu et al., 2019). On the other hand, the high acidity increases the bioavailability of PTEs and can affect microbial activity, community structure, and nutrient production (Baek et al., 2021; Munyai et al., 2021). For example, toxic metals including Cd, Cr, and Pb, and excessive amounts of metals Cu, Mn, Ni, and Zn, retard the growth of vegetables and have chronic effects on humans including kidney damage, cardiovascular failure, anaemia, and cancer (Edelstein and Ben-Hur, 2018).

Many studies regarding the metal types, sources, and pollution status of farmland topsoil in mining areas have been investigated (Zhao et al., 2021). It is found that both geological background and mining activities contribute to the high metal levels in mining areas (Wang et al., 2020). Given the potential remobilization of accumulated metals, these acidic soils can be considered a secondary pollution source (Amnai et al., 2021). Therefore, both the waste rocks and their surrounding soils need to be treated if their environmental risk is high (Tabelin et al., 2020; Ódri et al., 2020). To the best of our knowledge, few studies on soil environmental quality around waste rock heaps influenced by ARD were conducted.

China is one of the countries rich in pyrite resources with ore reserves of 540 million tons and more than 700 pyrite-mining areas. As reported, most pyrite deposits are of low sulfur content and are associated with a variety of other metallic minerals (e.g., galena) (Zhang et al., 2022). In this study, we took an abandoned pyrite mining area as an example to study the pollution status and environmental risks of the soil around waste rock heaps influenced by ARD. The main contents include: 1) characterizing the size of waste rock heaps and the content of PTEs in waste rocks; 2) investigating the concentration and pollution load change of PTEs in ARD in different seasons; and, 3) assessing the environmental risks of PTEs in the soil around waste rock heaps. This research will provide a more comprehensive understanding of the properties and effects of ARD in the pyrite mining area which is useful for the development of a sustainable control strategy of environmental pollution in waste pyrite mining areas.

2 Study area

The abandoned pyrite mining area, located in Baihe County (northwest China), covers a total area of 200 km^2. The pyrite deposits herein are controlled by the hydrothermal alteration of volcaniclastics. Pyrite mining activities commenced in the 1950s and ceased in 2000. According to local meteorological statistics, this area is subjected to a typical subtropical continental monsoon climate with a mean annual temperature of 15.6°C. The rain-fall is strong and seasonal with a mean annual value of 1,050 mm (mostly in June, July, August, and September). Based on the catchment area of different creeks, the mining area can be divided into four zones, namely Zone A, Zone B, Zone C, and Zone D. As shown in Figure 1, Creeks A, B, C, and D all flow into the Baishi River, which enters into the Han River, 44 km away. The Han River is the water source of the middle route of the National South-to-North Water Diversion Project, so it is important to ensure that its water quality meets national requirements.

The study area is in the mid-and high-elevation mountains with deep valleys, steep peaks, and a slope of more than 30°. As shown in Table 1, a total of 35 waste rock heaps and

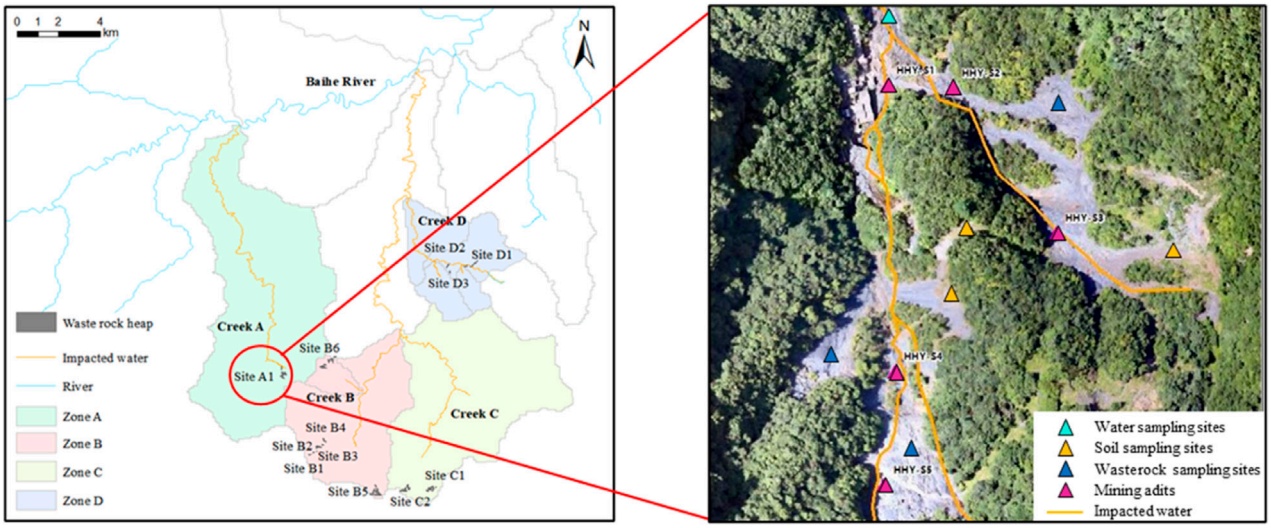

FIGURE 1
The layout of the abandoned pyrite mining area and the sampling locations in Site A1>.

TABLE 1 Number of waste rock heaps and abandoned mine adits in the abandoned pyrite mining area.

Catchment area	Mining sites	Waste rock heaps	Total number of abandoned mining adits
Creek A	Site A1	A1-I, A1-II, A1-III, A1-IV, A1-V, A1-VI, A1-VII, A1-VIII	22
Creek B	Site B1~B6	B1-I, B2-I, B2-II, B3-I, B3-II, B4-I, B5-I, B5-II, B5-III, B6-I, B6-II, B6-III, B6-IV, B6-V	68
Creek C	Site C1~C2	C1-I, C1-II, C1-III, C2-I, C2-II, C2-III, C2-IV	36
Creek D	Site D1~D3	D1-I, D2-I, D2-II, D3-I, D3-II,D3-III	46

172 abandoned mining adits were identified in the pyrite mining area. Up to now, waste rock was directly piled on the slope and the mining adits were open. Under the action of oxidation and rain leaching, the generated ARD with elevated concentrations of Fe, Mn, and other metal (loid)s ions keep flowing into the nearby water bodies, degrading water quality downstream and affecting the surrounding farmland. Based on information collected by drones in Sep. 2020, the total length of the impacted waterbody, which is yellow and muddy, is more than 55 km.

3 Materials and methods

3.1 Characterization of waste rock heaps

The volume of waste rock heaps was measured and calculated by the high-density resistance method (HDRM). HDRM in working is the same as the conventional resistivity method in principle, but it in observing is set higher density measured points on the layout of the electric poles on certain interval measuring points (Wu et al., 2016). Therefore, it has some advantages as follows: 1) several layouts of the electrodes could be designed and all arrangements detecting electrodes could be finished at one time; 2) the detected data can be collected and stored automatically; 3) the result of detected data could be interpreted easily (Ma and Du, 2014). At the same time, due to high resolution (0.5 m) satellite remote sensing image data, the location, floor area, quantity, and other attributes of waste rock heaps were also extracted.

3.2 Collection of waste rock, wastewater, and soil samples

To characterize the total content and leachability of PTEs of waste rock, at least two samples were collected from each waste rock heap and the sampling depth was set at least 4 m below the ground surface. A total of 79 waste rock samples were collected from 35 waste rock heaps.

For soil samples, sampling points were selected based on the size and the shape of waste rock heaps, as well as the sign of pollution. The sampling depth was determined based on the highest screening values of soil heavy metals by portable X-ray fluorescence (XRF). A total of 119 soil samples on the edges (approximately 5 m close to waste rock heaps) and downstream of the waste rock heap (within 200 m) were collected. In addition, 20 soil samples were collected from areas not affected by mining activities. After removing the surface waste residue or fallen leaves, a portable shovel was used to drill into the bedrock manually to a maximum drilling depth of 0.5 m.

In the study area, acidic effluents from all 12 mining sites flow down the valleys. A total of 24 ARD samples were collected located at the main discharge outlet of the mining site in both the rainy season (early September 2020) and dry season (late November 2020). The pH value and flow velocity were measured in the field, while parameters such as Cu, Zn, Cd, Pb, Cr, Ni, As, Fe, Mn, F^-, and SO_4^{2-} were measured in the laboratory.

3.3 Metal quantification of waste rock, acid rock drainage, and soil samples

For waste rock samples, the main elements were tested by the method of *Microbeam analysis-Quantitative analysis using energy dispersive spectrometry* (GBT 17359–2012), while the trace elements were tested by portable XRF (HD Rocksand). For soil samples, the microwave acid digestion method was used to measure the bulk of PTEs levels. In detail, soil samples of 0.5 g were placed in PVC digestion containers and digested with a 10 ml mixture of HCl, HF, and HNO_3. The digested solutions were diluted with 2% HNO_3 to a final volume of 50 ml.

The metals (e.g., As, Cd, Cr, Cu, Fe, Mn, Pb, Ni, and Zn) in ARD and digested solutions were tested by inductively coupled plasma mass spectrometry ICP-MS(Thermo Scientific, iCAP6300, United States), while the anions, F- and SO_4^{2-} were determined by ion chromatography (IC) (Thermo Scientific, Dionex ICS-1100, United States).

3.4 Leaching toxicity determination of waste rock and soil samples

To determine the leachability of PTEs in waste rock and soil samples, the Chinese Standard Solid Waste Extraction Procedure for Leaching Toxicity–Sulphuric Acid and nitric acid Method (HJ/T299-2007) and the Solid waste-Extraction procedure for leaching toxicity–Horizontal vibration method (HJ 557–2010) were performed. By comparing the limits regulated in Identification standards for hazardous wastes-Identification for extraction toxicity (GB 5085.3 -- 2007), the HJ/T299—2007 method is commonly used in China to determine whether solid waste is hazardous waste. In this method, a mixture of sulfuric acid and nitric acid (mass ratio 1:2) with a pH value of 3.20 ± 0.05 is used. In detail, 10.00 g (dry weight) of solid samples were extracted using the mixture acid at a liquid-to-solid (L/S) ratio of 10 (ml/g) for 18 h with a rotary tumber at 30 ± 2 r/min at ambient temperature. By comparing to the limits regulated in the Integrated wastewater discharge Standard GB 8978–1996 the HJ 557–2010 method is commonly used in China to assess the impact of solid waste on surface water. In detail, 10.00 g (dry weight) of solid samples were extracted using deionized water at an L/S ratio of 10 (ml/g) for 8 h with a water bath shock box at ambient temperature. The fluctuating frequency was 110 counts/min, and the amplitude was 40 mm.

All the eluates were filtered into a 15-ml polyethylene centrifugal tube by a 0.22-μmpore size syringe filter and then acidified by nitric acid to pH<2 (Li et al., 2021). The concentrations of Cu, Zn, Cd, Pb, Cr, Ni, and As in the supernatant were measured by ICP-MS.

3.5 Metal fractionation of soil samples

To investigate the different chemical speciation and the bioavailability of potentially toxic metals in soil samples, the modified three-step BCR sequential extraction method with additional pseudo-total digestion was adopted. In the BCR procedure, the acid-soluble fraction (F1) refers to the number of metals that can release into the environment when conditions become acidic (Pan et al., 2022). The reducible fraction (F2) represents the concentration of metals bound to iron and manganese oxides that can be released if substrates are exposed to more reductive conditions. The oxidizable fraction (F3) is generally considered to represent metals that are incorporated in stable, high molecular weight humic substances or occur as oxidizable minerals, e.g., sulfides, and is not considered to be very mobile or bioavailable. The details to assess the acid-soluble, reducible, oxidizable, and residual factions are described in previous studies (Spanka et al., 2018; Tong et al., 2020).

The concentrations of Cu, Cr, Pb, Zn, Ni, Pb, Cd, and As in the eluates for each step were tested by ICP-MS (diluted by nitric acid to pH<2, if necessary). The internal standard (ISTD) solution containing Sc, Ge, Rh, In, Tb, and Bi was prepared from Agilent's Internal Standard Mix (P/N: 5188–6525) using a 5% (v/v) nitric acid solution. Serving as an internal benchmark for the BCR sequential extraction procedure, the recovery efficiency is determined by comparing the sum of the four fractions (F1, F2, F3, and F4) with the total content of metals.

3.6 Data analysis and quality control

To ensure the data quality, all experiments/treatments were replicated at least two times. All data were reported as mean ±

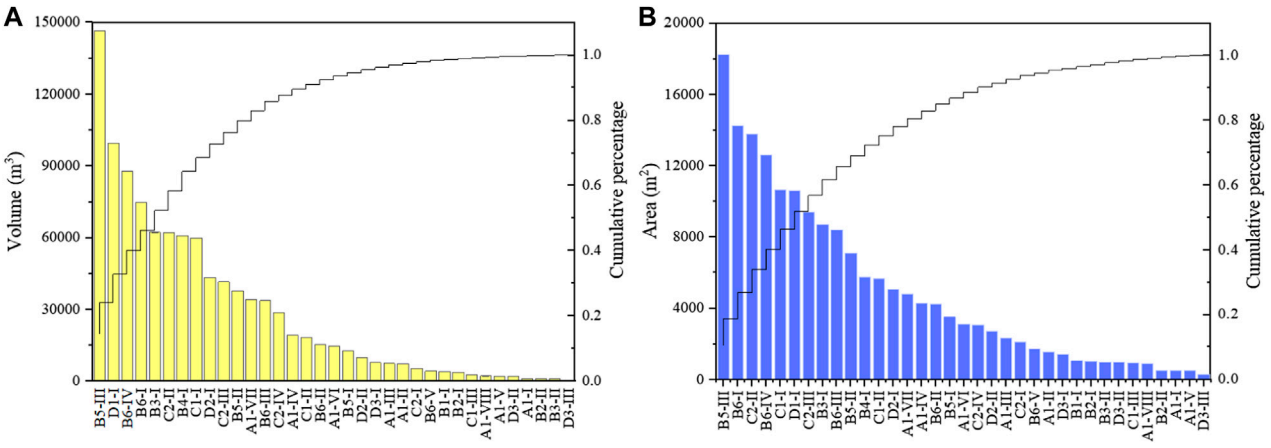

FIGURE 2
The volume **(A)** and area **(B)** of the waste rock heaps.>.

standard error of the mean (S.E.) unless stated otherwise. The recovery efficiencies of the targeted metals of soil samples were within 84.5% to 115.8%, indicating the metal fractionation is reliable and provides good repeatability. Also, Origin lab 2022 was used for correlation analysis in this study.

4 Results and discussion

4.1 Characteristics of waste rock and waste rock heaps

4.1.1 The size of waste rock heaps

The measurement results of the volumes and projected areas of 35 waste rock heaps are shown in Figure 2. The total volume and projected area of the waste rock heaps were 1,016,807 m^3 and 172,914 m^2, respectively. The average values of volume and projected area were 29,052 m^3 and 4,940 m^2, respectively. Based on field investigation, the maximum slope of 24 waste rock heaps was greater than or equal to 45°, while only 11 waste rock heaps were piled on a gentle slope (less than 45°). Considering that the waste rock pile is relatively loose, the waste rock on the hillside may not only have a higher risk of landslide but also be more likely to contaminate the surrounding soil (Zarroca et al., 2021).

By further comparing the size of different waste rock heaps, it was found that the volume of the top three waste rock heaps was 146,582 m^3 (B5-III), 99,420 m^3 (D1-I), and 87,813 m^3 (B6-IV), and the total accumulated contribution rate was 32.83%. In addition, the projected area of the top three waste rock heaps was 18,234 m^2 (B5-III), 14,253 m^2 (B6-I), and 13,787 m^2 (C2-II), and the total accumulated contribution rate was 26.76%. The maximum slope of the steepest three waste rock heaps was 73° (B5-III), 73° (C1-I), and 67° (C2-I). It is worth noting that the B5-III had the highest values of volume, size, and maximum slope in all the waste rock heaps. Hence, to reduce the pollution caused by waste rocks, onsite or offsite treatment strategies, should be compared according to the size, slope, and hydrogeological conditions of waste rock heaps.

4.1.2 The bulk of common and trace elements in waste rocks

As shown in Figures 3A, Si, Al, K, and O are the main elements identified in waste rocks. This is consistent with field observations and previous reports that the minerals in the waste rock of pyrite deposits are mainly pyroxene and feldspar, with a small amount of quartz and green mud (Xie et al., 2020). Also, the bulk S level as high as 0.86%, indicated that waste rocks own a high acid production capacity (Gerson et al., 2019). Usually, pyrite is often associated with a variety of metallic elements including Pb, Zn, and Cu (Dold, 2017). The bulk of Ni, As, Cd, Cu, Pb, Cr, and Zn in waste rock was 29, 32, 35, 41, 65, 81, and 122 mg kg^{-1}, respectively. Even if a relatively low content of PTEs in this area, in case of improper disposal of pyrite mining wastes, waste rocks might leach out and cause potential risks to the surrounding environment (Tabelin et al., 2017). Besides, as F is the 13th most abundant element in the Earth's crust, relatively high content of F was identified in the waste rocks of this study.

4.1.3 Metal leaching behavior from waste rocks

The results of leaching tests for all 79 waste rock samples are shown in Figure 4. The metal leaching concentrations followed by HJ/T299-2007 range from 0.1 mg/L to 1.5 mg/L, below the limits regulated in GB 5085.3 -- 2007, indicating the waste rocks were not hazardous wastes. According to relevant Chinese regulations, such solid waste does not need to be disposed of in hazardous waste

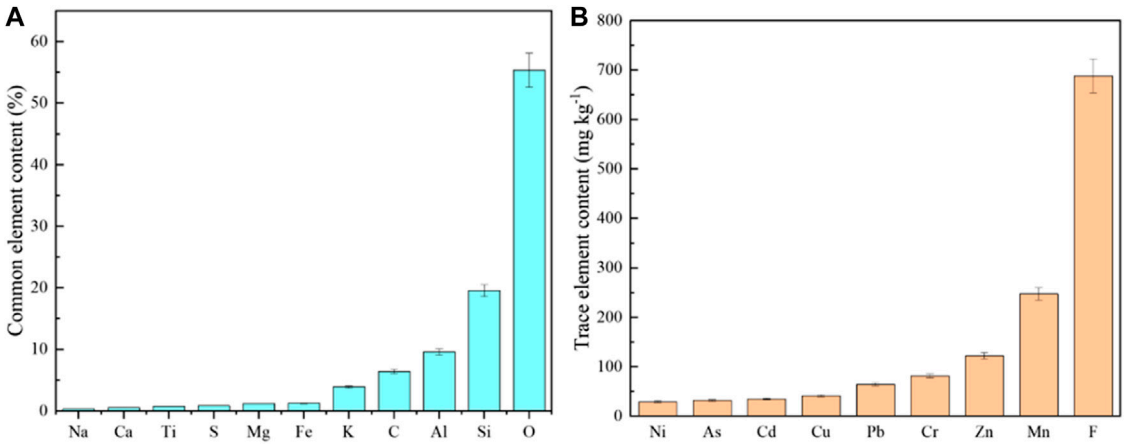

FIGURE 3
The major **(A)** and trace **(B)** element content in waste rocks.

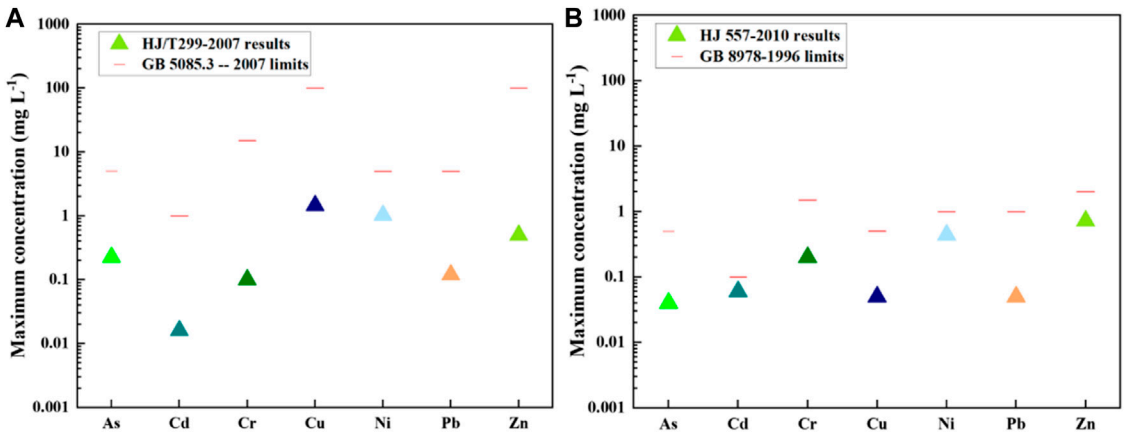

FIGURE 4
The maximum PTEs leaching concentrations in waste rocks followed by different leaching tests **(A)** HJ/T299-2007 and **(B)** HJ 557-2010.

landfills. The metal leaching results followed by HJ 557–2010 range from 0.04 mg/L to 0.72 mg/L, below but very close to the limits regulated in GB 8978–1996, informing the metals in waste rock have a potentially significant risk of impact on surface water. Given the acidic pH of the leaching solution, the waste rock needs to be further treated.

4.2 Properties of the acid rock drainage

The concentration of metal (loid)s, sulfate, and fluoride, as well as the pH value of ARD samples, collected in the rainy season and dry season, are shown in Figure 5. All ARD samples in 12 mining sites were highly acidic in both the rainy season (pH: 1.72–2.54) and the dry season (pH: 1.72–2.47), indicating that the rainy season will lead to more acidic ARD discharge, and impact the surrounding soil to a greater extent. Except for Ni, the average concentration of Cu, Zn, Cd, Pb, Cr, As, Fe, Mn, F^-, and SO_4^{2-} in the samples of the dry season was higher than that in the rainy season. According to the field measurement, the flow velocity of ARD at the discharge outlet of the 12 mining sites in the rainy season and the dry season was 2.16 L/s and 1.39 L/s, respectively. The dilution from rainwater can reduce their concentrations, but may lead to a more pronounced effect on the surrounding soil due to the rising water levels and flow velocities (Engel et al., 2021; Gomes et al., 2022).

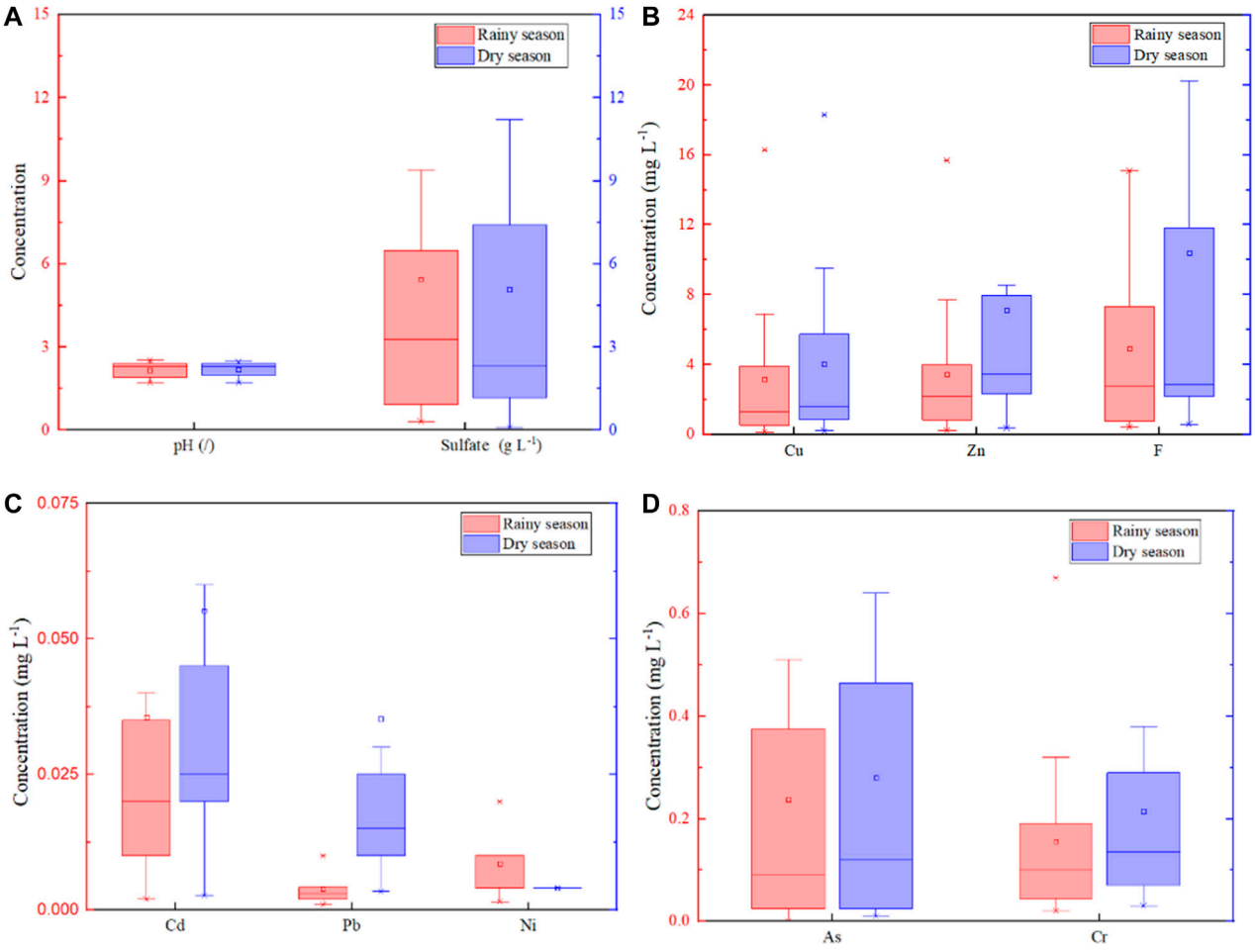

FIGURE 5
Comparison of the pH value and the concentration change of Sulfate **(A)**, Cu, Zn, and F **(B)**, Cd, Pb, and Ni **(C)**, As, and Cr **(D)** in 24 ARD samples in different seasons.

Usually, Fe and Mn have fewer side effects on human health than the aforementioned pollutants. While considering Fe and Mn can change the properties of water, especially causing sensory problems, many countries regulate the content of Fe and Mn in water (Huang et al., 2015; Khadse et al., 2015). As shown in Figure 6A, the changes in Fe and Mn concentrations in different seasons were in line with other pollutants, with higher levels during the dry season. However, as the flow increases, so does the pollution load during the rainy season. As shown in Figure 6B, the pollution load of Mn in the dry season and the rainy season was 12.4 mg/s and 18.7 mg/s, respectively. The pollution load of Fe in the dry season and the rainy season was 795 mg/s and 1,172 mg/s, respectively. Overall, the load in the rainy season was about 1.5 times that in the dry season, indicating that acidic wastewater may have a greater impact on the surrounding soil under rainy season conditions.

4.3 Environmental quality of soil around waste rock heaps

4.3.1 The bulk of potentially toxic elements

The bulk of PTEs and pH values of soil samples, as well as their descriptive statistics results, are presented in Table 2. As shown, the average values of Ni, Cu, Pb, Zn, Cd, As, Cr and Mn in soil samples are higher than the corresponding background values, which shows that these pollutants are enriched in the soil to different degrees. Also, It was found that more than 70% of the 119 soil samples were acidic (pH<5.5), and more than 30% of which were strongly acidic (pH<4.7).

As no available evaluation standards for soil pollution in mining areas were identified, The *Soil environmental quality - Risk control standard for soil contamination of development land (GB36600 -- 2018)* was further used to preliminarily evaluate the possible human health risks of Ni, Cu, Pb, Zn, Cd, As, Cr. As

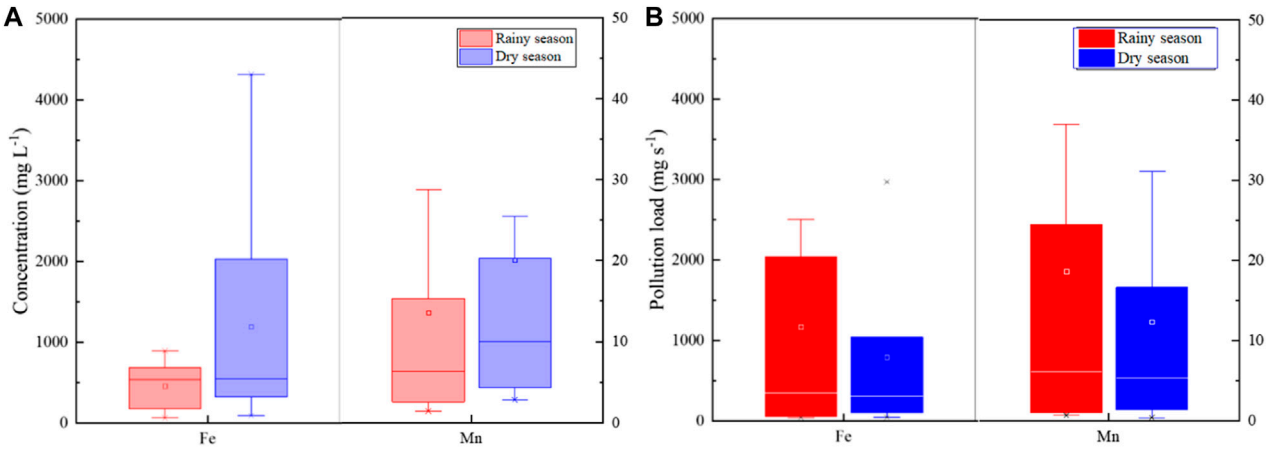

FIGURE 6
Comparison of the concentration **(A)** and pollution load **(B)** change for Fe and Mn in 24 ARD samples in different seasons.

TABLE 2 Descriptive statistics of the soil PTE concentrations in the study area.

Parameter	pH	As	Cd	Cr	Cu	Mn	Ni	Pb	Zn	F	Fe
Unit	—	mg kg^{-1}	mg kg^{-1}	mg kg^{-1}	mg kg^{-1}	mg kg^{-1}	mg kg^{-1}	mg kg^{-1}	mg kg^{-1}	mg kg^{-1}	%
Average value	4.82	39.9	0.98	87.2	100	875	60.7	36.7	161	654	6.02
Minimum value	2.6	6.0	0.01	28.0	19.0	50.0	6.0	10.0	35.0	288	2.1
Maximum value	8.2	369	10.8	431	1,006	4364	265	160	612	1846	33.4
Median	4.62	30.9	0.41	84	74	756	46	30	131.5	608	5.35
standard deviation	1.36	38.97	1.65	49.04	113.38	609.35	48.39	20.39	109.24	212.06	3.26
variable coefficient	0.28	0.98	1.68	0.56	1.13	0.70	0.80	0.56	0.68	0.32	0.54
Background value in study area	8.70	15.2	0.150	87.7	35.4	758	40.4	30.5	108	827	4.15
Background value in China	—	11.2	0.097	61.0	22.6	583	26.9	26.0	74.2	—	—
GB36600 -- 2018	NA	60	65	NA	18000	NA	900	800	NA	NA	NA

NA, not applicable; GB36600 -- 2018 = Soil environmental quality-Risk control standard for soil contamination of development land.

shown in Table 2, the contents of PTEs in the soil of the mining area vary greatly. A total of 17 samples were found to have As levels exceeding the limit of 60 mg kg^{-1}. Among them, only one soil sample had arsenic content over 300 mg/kg, and the rest samples had arsenic content of less than 100 mg/kg. The GB36600—2018 sets these limits for heavy metal concentrations in soil based on the protection of human health in construction land scenarios. Under conditions used as construction land, heavy metals can enter the body through oral ingestion of soil, skin contact with soil, and inhalation of soil particles. However, in this study area, waste rock heaps are located in a remote location with limited exposure pathways and receptors. Therefore, the human health risk of the soil surrounding the waste heaps appears to be generally acceptable.

4.3.2 Metal leaching behavior from contaminated soil

The potential risk of PTEs in soils, concerning their mobility and ecotoxicological significance, is determined by their solid-solution partitioning rather than the total heavy metal content (Dijkstra et al., 2004). All 17 soil samples with relatively higher As concentrations were selected to perform the leaching tests. As presented in Figure 7A, the metal leaching concentration of all samples followed by HJ/T299-2007 ranges from 0.01 mg/L to 0.34 mg/L, far below the limits regulated in GB 5085.3 -- 2007, indicating the soil surrounding the waste rock heaps area was not hazardous waste. Also, as shown in Figure 7B, the metal leaching results followed by HJ 557–2010 range from 0.01 mg/L to 0.12 mg/L, all below the limits regulated in GB

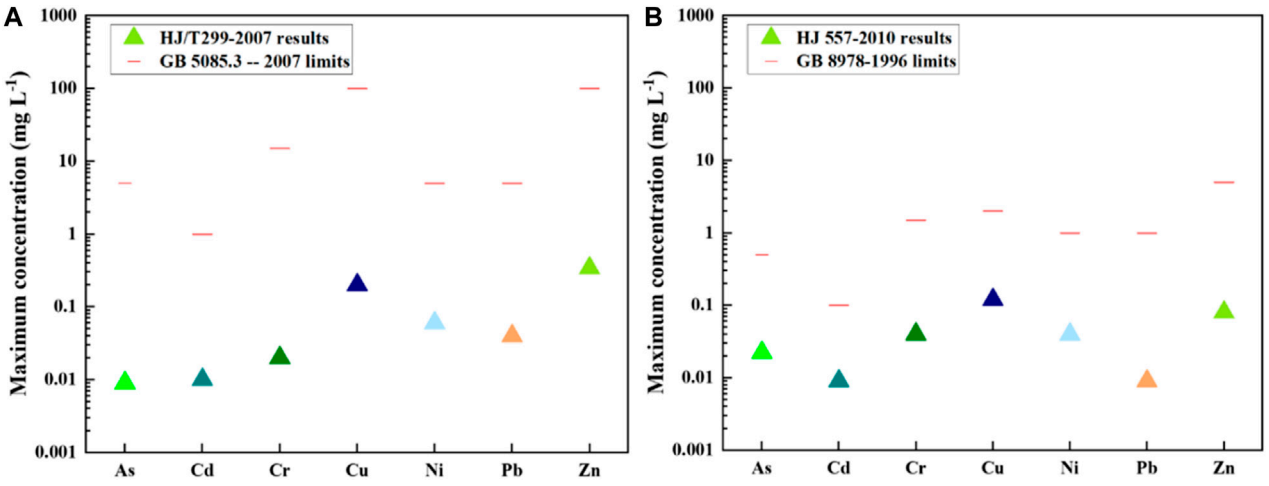

FIGURE 7
The maximum PTEs leaching concentrations in 17 contaminated soil samples followed by different leaching tests **(A)** HJ/T299-2007 and **(B)** HJ 557-2010.

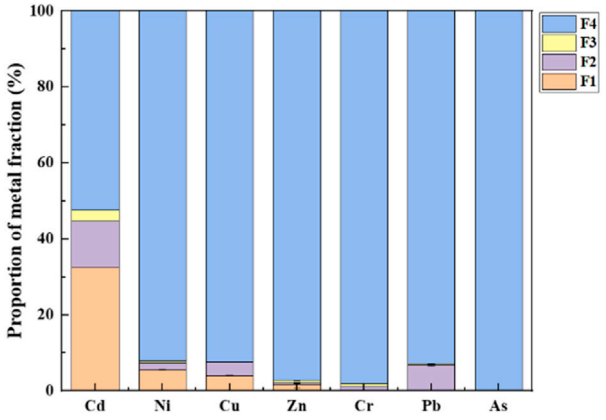

FIGURE 8
The BCR sequential extraction results of trace toxic metals.

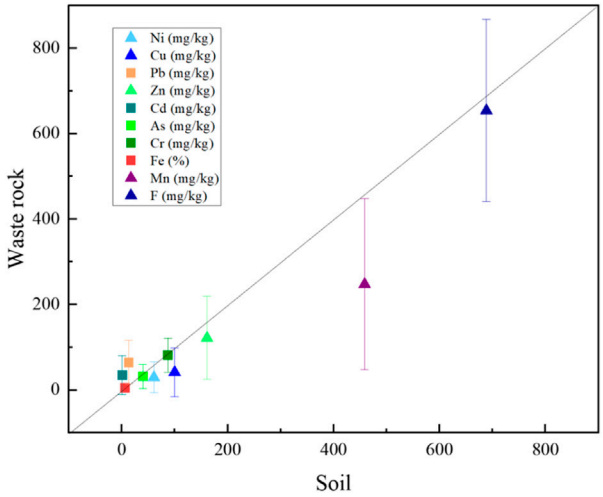

FIGURE 9
Comparison of PTEs contents in soil and waste rock.

8978–1996 informing the metals enriched in soil are relatively stable.

4.3.3 Chemical speciation of potentially toxic elements in contaminated soil

To further explain the leaching test results, the speciation of metals (Ni, Cu, Pb, Zn, Cd, As, and Cr) in the soil sample with the highest As content (369 mg/kg) was analyzed through the modified BCR sequential extraction procedure. As shown in Figure 8, except for Cd, the residual fraction of other metals in the soil accounted for over 90%. Generally, the residual fraction consists of primary and secondary silicates and minerals, which can retain elements within the crystalline structures (Zhao et al., 2020). Thus, arsenic with 99.9% occurring in the residual fraction is not considered to be available to the environment in natural conditions. As reported by previous studies, many kinds of iron-bearing minerals have been found in the soil of mining areas, such as Schwertmannite and goethite, and these minerals have good performance in the stabilization of As (Amnai et al., 2021). Considering the relatively low bioavailability of PTEs and limited exposure routes, the human health risk of the soil surrounding the waste heap is generally acceptable.

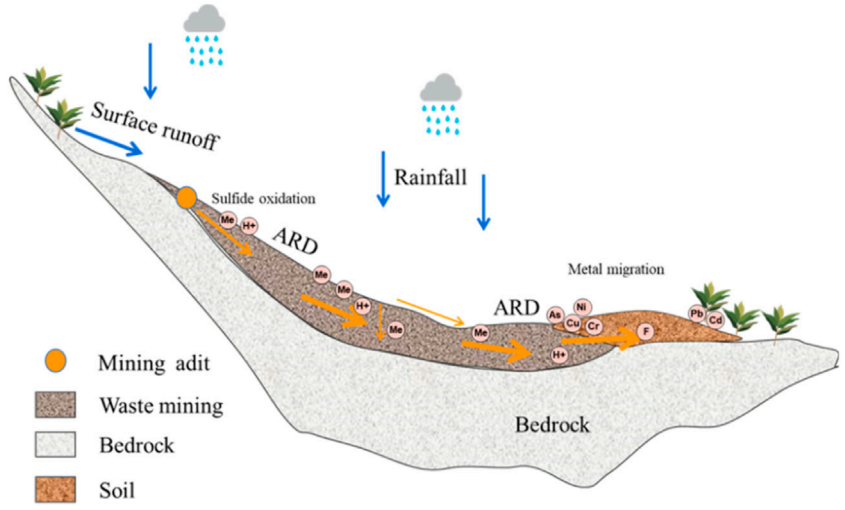

FIGURE 10
Conceptual site model in the abandoned pyrite mining area.

4.4 Mechanisms of acid rock drainage influencing soil quality

The mechanisms of ARD influencing soil quality in mining areas are very complicated (Pan et al., 2022). In this study area, most of the soil samples were acidic, some were strongly acidic and extremely acidic, indicating that soil around and downstream of the waste rock heaps was already affected by ARD to a certain extent. The occurrence and migration of PTEs are further affected by their chemical speciation and their affinity to bind to reactive surfaces in the soil matrix and pore water [such as particulate and dissolved organic matter, clays, or metal (hydr) oxide surfaces] (Zhao et al., 2017; Li et al., 2019). For example, Fe and Cu prefer to bind with humic-like DOM while Zn prefers to bind with protein-like DOM (Liu et al., 2021), and As prefers to bind with Fe-Mn bimetallic oxides (Xie et al., 2022).

To elucidate the effect of acidic ARD on soil, the difference in PTEs content between soils and waste rocks was compared. As shown in Figure 9, Ni, Cu, Zn, Mn, and F levels were higher in the soil samples, while Pb and Cd were higher in the waste rock samples. Fe, As, and Cr levels were found equal in soil and waste rocks. In general, the bulk F and Ni levels were mainly controlled by background values, while the lower Cd and Pb levels in the soils were close to waste rock heaps due to their strong mobility under acidic conditions. These two PTEs enter the soil from acidic ARD and migrate longer distances when washed by ARD in the rainy season (Zhang et al., 2021).

Based on the above discussion, a conceptual model of soil pollution around waste rock heaps was proposed in this study. As illustrated in Figure 10, the sulfides present in waste rock heaps, in contact with oxygen and environmental water, oxidize producing sulfuric acid. ARD solubilizes the solid minerals, producing a liquid containing dissolved metals and sulfuric acid, which can impact the surrounding soil. Though the high contents of elements in the mining area result from the regional geological background, the high bulk PTEs in this study were mainly caused by ARD. In addition, some metals (e.g., Pb and Cd) in acidified soils migrate longer distances under rain-washed conditions (Engel et al., 2021; Gomes et al., 2022).

5 Conclusion

Coupling the findings from field investigation and statistical analysis, we may conclude that waste rock in the abandoned pyrite mining area continues to produce a steady stream of acidic ARD for decades. The concentrations of PTEs (including pH, As, Cd, Cu, Fe, Mn, Zn, and F) in ARD were very high both in the rainy season and dry season. Hence it is necessary to take some action, such as passivation technology for waste rocks, to reduce the generation of acid wastewater. Serious soil acidification was found in more than 70% of the sampling points around the waste rock heaps. Many elements were enriched in the soil, and the As concentrations exceeded the national standard. However, the leaching concentration of heavy metals in the soil ranges from 0.01 mg/L to 0.72 mg/L, below the respective regulated limits. According to the metal fractionation results, heavy metals mainly occur in a stable state, e.g., retained in the solid matrix in soil. Due to the acceptable human health risk, the soil surrounding the waste rock heaps does not need to be treated as hazardous waste, and green and sustainable remediation techniques, such as soil improvement and phytoremediation are suggested. The results of the study may be referred to by various stakeholders, including mining industries, local governments, and environmental consulting companies, to integrate

them into their post-mining measures, thereby making them aware of the potential long-term impact of ARD generated from waste rocks on soil quality and human health.

Data availability statement

The raw data supporting the conclusions of this article will be made available by the authors, without undue reservation.

Author contributions

LZ contributed to data collection, methodology, writing-original draft, and writing-review and editing; XP and DC contributed to field investigation, methodology; WW and XL contributed to reviewing and editing. All authors have read and agreed to the published version of the manuscript.

Funding

This study was financed by the Fundamental Program of the Special Scientific Research Fund of Central Public Welfare Scientific Research Institutes (No. PM-zx097-202104-072), Guangzhou Science and Technology Programme (No. PM-zx278-202105-158), and the Youth Innovation Fund of Eco-environment Remediation Research Center, SCIES (No. hx_202109_002).

Acknowledgments

Also, the authors would like to thank BGRIMM Technology Group and Shannxi Geology and Mining Group for their help in the fieldwork and laboratory analysis.

Conflict of interest

The authors declare that the research was conducted in the absence of any commercial or financial relationships that could be construed as a potential conflict of interest.

Publisher's note

All claims expressed in this article are solely those of the authors and do not necessarily represent those of their affiliated organizations, or those of the publisher, the editors and the reviewers. Any product that may be evaluated in this article, or claim that may be made by its manufacturer, is not guaranteed or endorsed by the publisher.

References

Alekseyev, V. A. (2022). Reasons for the formation of acidic drainage water in dumps of sulfide-containing rocks. *Geochem. Int.* 60, 78–91. doi:10.1134/s0016702922010025

Amnai, A., Radola, D., Choulet, F., Buatier, M., and Gimbert, F. (2021). Impact of ancient iron smelting wastes on current soils: Legacy contamination, environmental availability and fractionation of metals. *Sci. Total Environ.* 776, 145929. doi:10.1016/j.scitotenv.2021.145929

Baek, I., Kim, J., Song, Y., and Kim, T. (2021). Neutralization effect of slag on the acid rock drainage. *Int. J. Geoeng.* 12, 2. doi:10.1186/s40703-020-00131-2

Casagrande, M. F. S., Moreira, C. A., and Targa, D. A. (2019). Study of generation and underground flow of acid mine drainage in waste rock pile in an uranium mine using electrical resistivity tomography. *Pure Appl. Geophys.* 177, 703–721. doi:10.1007/s00024-019-02351-9

Dijkstra, J. J., Meeussen, J. C., and Comans, R. N. (2004). Leaching of heavy metals from contaminated soils: An experimental and modeling study. *Environ. Sci. Technol.* 38, 4390–4395. doi:10.1021/es049885v

Dold, B. (2017). Acid rock drainage prediction: A critical review. *J. Geochem. Explor.* 172, 120–132. doi:10.1016/j.gexplo.2016.09.014

Edelstein, M., and Ben-Hur, M. (2018). Heavy metals and metalloids: Sources, risks and strategies to reduce their accumulation in horticultural crops. *Sci. Hortic.* 234, 431–444. doi:10.1016/j.scienta.2017.12.039

Engel, M., Lezama Pacheco, J. S., Noel, V., Boye, K., and Fendorf, S. (2021). Organic compounds alter the preference and rates of heavy metal adsorption on ferrihydrite. *Sci. Total Environ.* 750, 141485. doi:10.1016/j.scitotenv.2020.141485

Fan, R., Short, M. D., Zeng, S. J., Qian, G., Li, J., Schumann, R. C., et al. (2017). The formation of silicate-stabilized passivating layers on pyrite for reduced acid rock drainage. *Environ. Sci. Technol.* 51, 11317–11325. doi:10.1021/acs.est.7b03232

Gerson, A. R., Rolley, P. J., Davis, C., Feig, S. T., Doyle, S., and Smart, R. S. C. (2019). Unexpected non-acid drainage from sulfidic rock waste. *Sci. Rep.* 9, 4357. doi:10.1038/s41598-019-40357-4

Gomes, T., Angioletto, E., Quadri, M. B., Cargnin, M., and de Souza, H. M. (2022). Acceleration of acid mine drainage generation with ozone and hydrogen peroxide: Kinetic leach column test and oxidant propagation modeling. *Miner. Eng.* 175, 107282. doi:10.1016/j.mineng.2021.107282

Huang, B., Li, Z., Chen, Z., Chen, G., Zhang, C., Huang, J., et al. (2015). Study and health risk assessment of the occurrence of iron and manganese in groundwater at the terminal of the Xiangjiang River. *Environ. Sci. Pollut. Res.* 22, 19912–19921. doi:10.1007/s11356-015-5230-z

Khadse, G. K., Patni, P. M., and Labhasetwar, P. K. (2015). Removal of iron and manganese from drinking water supply. *Sustain. Water Resour. Manag.* 1, 157–165. doi:10.1007/s40899-015-0017-4

Li, D., Xie, L., Carvan, M. J., 3rd, and Guo, L. (2019). Mitigative effects of natural and model dissolved organic matter with different functionalities on the toxicity of methylmercury in embryonic zebrafish. *Environ. Pollut.* 252, 616–626. doi:10.1016/j.envpol.2019.05.155

Li, Z., Ma, G., Zhang, X., and Li, J. (2021). Characteristics and chemical speciation of waste copper slag. *Environ. Sci. Pollut. Res.* 28, 20012–20022. doi:10.1007/s11356-020-11830-9

Liu, J., Li, N., Zhang, W., Wei, X., Tsang, D. C. W., Sun, Y., et al. (2019). Thallium contamination in farmlands and common vegetables in a pyrite mining city and potential health risks. *Environ. Pollut.* 248, 906–915. doi:10.1016/j.envpol.2019.02.092

Liu, M., Han, X., Liu, C. Q., Guo, L., Ding, H., and Lang, Y. (2021). Differences in the spectroscopic characteristics of wetland dissolved organic matter binding with Fe3+, Cu2+, Cd2+, Cr3+ and Zn2+. *Sci. Total Environ.* 800, 149476. doi:10.1016/j.scitotenv.2021.149476

Ma, D. X., and Du, R. Q. (2014). Three-dimensional inversion and visual expression of two-dimensional data in high density resistivity method. *Appl. Mech. Mater.* 644-650, 1377–1381. doi:10.4028/www.scientific.net/amm.644-650.1377

Ma, L., Huang, C., Liu, Z. S., Morin, K. A., Aziz, M., and Meints, C. (2019). Prediction of acid rock drainage in waste rock piles Part 1: Water film model for geochemical reactions and application to a full-scale case study. *J. Contam. Hydrology* 220, 98–107. doi:10.1016/j.jconhyd.2018.11.012

Munyai, R., Ogola, H. J. O., and Modise, D. M. (2021). Microbial community diversity dynamics in acid mine drainage and acid mine drainage-polluted soils: Implication on mining water irrigation agricultural sustainability. *Front. Sustain. Food Syst.* 5. doi:10.3389/fsufs.2021.701870

Naidu, G., Ryu, S., Thiruvenkatachari, R., Choi, Y., Jeong, S., and Vigneswaran, S. (2019). A critical review on remediation, reuse, and resource recovery from acid mine drainage. *Environ. Pollut.* 247, 1110–1124. doi:10.1016/j.envpol.2019.01.085

Ódri, Á., Becker, M., Broadhurst, J., Harrison, S., and Edraki, M. (2020). Stable isotope imprints during pyrite leaching: Implications for acid rock drainage characterization. *Minerals* 10, 982. doi:10.3390/min10110982

Olenici, A., Blanco, S., Borrego-Ramos, M., Momeu, L., and Baciu, C. (2017). Exploring the effects of acid mine drainage on diatom teratology using geometric morphometry. *Ecotoxicology* 26, 1018–1030. doi:10.1007/s10646-017-1830-3

Pan, Y., Fu, Y., Liu, S., Ma, T., Tao, X., Ma, Y., et al. (2022). Spatial and temporal variations of metal fractions in paddy soil flooding with acid mine drainage. *Environ. Res.* 212, 113241. doi:10.1016/j.envres.2022.113241

Plaza, F., Wen, Y., and Liang, X. (2018). Acid rock drainage passive remediation using alkaline clay: Hydro-geochemical study and impacts of vegetation and sand on remediation. *Sci. Total Environ.* 637-638, 1262–1278. doi:10.1016/j.scitotenv.2018.05.014

Plaza, F., Wen, Y., Perone, H., Xu, Y., and Liang, X. (2017). Acid rock drainage passive remediation: Potential use of alkaline clay, optimal mixing ratio and long-term impacts. *Sci. Total Environ.* 576, 572–585. doi:10.1016/j.scitotenv.2016.10.076

Spanka, M., Mansfeldt, T., and Bialucha, R. (2018). Sequential extraction of chromium, molybdenum, and vanadium in basic oxygen furnace slags. *Environ. Sci. Pollut. Res.* 25, 23082–23090. doi:10.1007/s11356-018-2361-z

Sulonen, M. L. K., Baeza, J. A., Gabriel, D., and Guisasola, A. (2021). Optimisation of the operational parameters for a comprehensive bioelectrochemical treatment of acid mine drainage. *J. Hazard. Mater.* 409, 124944. doi:10.1016/j.jhazmat.2020.124944

Tabelin, C. B., Sasaki, R., Igarashi, T., Park, I., Tamoto, S., Arima, T., et al. (2017). Simultaneous leaching of arsenite, arsenate, selenite and selenate, and their migration in tunnel-excavated sedimentary rocks: I. Column experiments under intermittent and unsaturated flow. *Chemosphere* 186, 558–569. doi:10.1016/j.chemosphere.2017.07.145

Tabelin, C. B., Silwamba, M., Paglinawan, F. C., Mondejar, A. J. S., Duc, H. G., Resabal, V. J., et al. (2020). Solid-phase partitioning and release-retention mechanisms of copper, lead, zinc and arsenic in soils impacted by artisanal and small-scale gold mining (ASGM) activities. *Chemosphere* 260, 127574. doi:10.1016/j.chemosphere.2020.127574

Tong, L., He, J., Wang, F., Wang, Y., Wang, L., Tsang, D. C. W., et al. (2020). Evaluation of the BCR sequential extraction scheme for trace metal fractionation of alkaline municipal solid waste incineration fly ash. *Chemosphere* 249, 126115. doi:10.1016/j.chemosphere.2020.126115

Wang, R., Deng, H., Yan, M. S., He, Z. X., Zhou, J., Liang, S. B., et al. (2020). Assessment and source analysis of heavy metal pollution in farmland soils in southern youyang county, chongqing. *Huan Jing Ke Xue Chin.* 41, 4749–4756. doi:10.13227/j.hjkx.202003175

Wu, G., Yang, G., and Tan, H. (2016). Mapping coalmine goaf using transient electromagnetic method and high density resistivity method in Ordos City, China. *Geodesy Geodyn.* 7, 340–347. doi:10.1016/j.geog.2016.04.014

Xie, J., Ge, L., Qian, L., Li, Q., and Sun, W. (2020). Trace element characteristics of pyrite in Dongguashan Cu (Au) deposit, Tongling region, China. *Solid Earth Sci.* 5, 233–246. doi:10.1016/j.sesci.2020.09.002

Xie, X., Lu, C., Xu, R., Yang, X., Yan, L., and Su, C. (2022). Arsenic removal by manganese-doped mesoporous iron oxides from groundwater: Performance and mechanism. *Sci. Total Environ.* 806, 150615. doi:10.1016/j.scitotenv.2021.150615

Zarroca, M., Roque, C., Linares, R., Salminci, J. G., and Gutierrez, F. (2021). Natural acid rock drainage in alpine catchments: A side effect of climate warming. *Sci. Total Environ.* 778, 146070. doi:10.1016/j.scitotenv.2021.146070

Zhang, J., Shi, Z., Ni, S., Wang, X., Liao, C., and Wei, F. (2021). Source identification of Cd and Pb in typical farmland topsoil in the southwest of China: A case study. *Sustainability* 13, 3729. doi:10.3390/su13073729

Zhang, Y., Shao, Y., Liu, Q., Zhang, X., Zhan, Y., Wang, C., et al. (2022). Pyrite textures, trace element and sulfur isotopes of Yanlinsi slate-hosted deposit in the Jiangnan Orogen, South China: Implications for gold mineralization processes. *Ore Geol. Rev.* 148, 105029. doi:10.1016/j.oregeorev.2022.105029

Zhao, L., Yan, Y., Yu, R., Hu, G., Cheng, Y., and Huang, H. (2020). Source apportionment and health risks of the bioavailable and residual fractions of heavy metals in the park soils in a coastal city of China using a receptor model combined with Pb isotopes. *Catena* 194, 104736. doi:10.1016/j.catena.2020.104736

Zhao, W., Gu, C., Ying, H., Feng, X., Zhu, M., Wang, M., et al. (2021). Fraction distribution of heavy metals and its relationship with iron in polluted farmland soils around distinct mining areas. *Appl. Geochem.* 130, 104969. doi:10.1016/j.apgeochem.2021.104969

Zhao, Y., Song, K., Wen, Z., Fang, C., Shang, Y., and Lv, L. (2017). Evaluation of CDOM sources and their links with water quality in the lakes of Northeast China using fluorescence spectroscopy. *J. Hydrology* 550, 80–91. doi:10.1016/j.jhydrol.2017.04.027

Zhou, Y., Fan, R., Short, M. D., Li, J., Schumann, R. C., Xu, H., et al. (2018). Formation of aluminum hydroxide-doped surface passivating layers on pyrite for acid rock drainage control. *Environ. Sci. Technol.* 52, 11786–11795. doi:10.1021/acs.est.8b04306